Received: 15 May 2017 | Revised: 30 October 2017 | Accepted: 14 November 2017

DOI: 10.1002/nla.2137

RESEARCH ARTICLE

WILEY

Eigenvalues and eigenvectors of banded Toeplitz matrices and the related symbols

S.-E. Ekström[1] | S. Serra-Capizzano[1,2]

[1]Department of Information Technology, Division of Scientific Computing, ITC, Uppsala University, Lägerhyddsv. 2, SE-751 05 Uppsala, Sweden

[2]Department of Science and High Technology, Insubria University, via Valleggio 11, Como 22100, Italy

Correspondence
S.-E. Ekström, Department of Information Technology, Division of Scientific Computing, ITC, Uppsala University, Lägerhyddsv. 2, P.O. Box 337, SE-751 05 Uppsala, Sweden.
Email: sven-erik.ekstrom@it.uu.se

Funding information
Graduate School in Mathematics and Computing (FMB); Uppsala University; Istituto Nazionale di Alta Matematica-Gruppo Nazionale di Calcolo Scientifico

Summary

It is known that for a tridiagonal Toeplitz matrix, having on the main diagonal the constant a_0 and on the two first off-diagonals the constants a_1 (lower) and a_{-1} (upper), which are all complex values, there exist closed form formulas, giving the eigenvalues of the matrix and a set of associated eigenvectors. For example, for the 1D discrete Laplacian, this triple is $(a_0, a_1, a_{-1}) = (2, -1, -1)$. In the first part of this article, we consider a tridiagonal Toeplitz matrix of the same form $(a_0, a_\omega, a_{-\omega})$, but where the two off-diagonals are positioned ω steps from the main diagonal instead of only one. We show that its eigenvalues and eigenvectors can also be identified in closed form and that interesting connections with the standard Toeplitz symbol are identified. Furthermore, as numerical evidences clearly suggest, it turns out that the eigenvalue behavior of a general banded symmetric Toeplitz matrix with real entries can be described qualitatively in terms of the symmetrically sparse tridiagonal case with real a_0, $a_\omega = a_{-\omega}$, $\omega = 2, 3, \dots$, and also quantitatively in terms of those having monotone symbols. A discussion on the use of such results and on possible extensions complements the paper.

KEYWORDS

eigensolver, generating function and spectral symbol, Toeplitz matrix

1 | INTRODUCTION

Let A_n be a Toeplitz matrix of order n and let $\omega < n$ be a positive integer, as follows:

$$A_n = \begin{bmatrix} a_0 & \cdots & a_{-\omega} & & & \\ \vdots & \ddots & & \ddots & & \\ a_\omega & & \ddots & & \ddots & \\ & \ddots & & \ddots & & a_{-\omega} \\ & & \ddots & & \ddots & \vdots \\ & & & a_\omega & \cdots & a_0 \end{bmatrix}, \tag{1}$$

with the coefficients a_k, $k = -\omega, \dots, \omega$, being complex numbers.

Let $f \in L^1(-\pi, \pi)$ and let $T_n(f)$ be the Toeplitz matrix generated by f, that is, $(T_n(f))_{s,t} = \hat{f}_{s-t}$, $s, t = 1, \dots, n$, with f being the generating function of $\{T_n(f)\}$ and with $\hat{f}_k$ being the kth Fourier coefficient of f, that is,

$$\hat{f}_k = \frac{1}{2\pi} \int_{-\pi}^{\pi} f(\theta) \quad e^{-\mathbf{i}k\theta} \, \mathrm{d}\theta, \quad \mathbf{i}^2 = -1, \quad k \in \mathbb{Z}. \tag{2}$$

If f is real valued, then several spectral properties are known (localization, extremal behavior, and collective distribution; see other works[1,2] and references therein), and f is also the spectral symbol of $\{T_n(f)\}$ in the Weyl sense.[1,3–5] If f is complex valued, then the same type of information is transferred to the singular values, whereas the eigenvalues can have a "wild" behavior[6] in some cases. According to the notation above, our setting is very special because by direct computation, the generating function of the Toeplitz matrix in (1) is the trigonometric polynomial $f(\theta) = \sum_{k=-\omega}^{\omega} a_k e^{\mathbf{i}k\theta}$, that is, $A_n = T_n(f)$.

In this paper, we are interested in quantitative estimates of the eigenvalues of A_n. Indeed, in the the band symmetric Toeplitz setting, quantitative estimates are already available in the relevant literature. In fact, using an embedding argument in the Tau algebra (the set of matrices diagonalized by a sine transform[7]), we are led to the conclusion that the jth eigenvalue $\lambda_j(A_n) = \lambda_{j,n}$, $A_n = T_n(f)$, $a_k = a_{-k} \in \mathbb{R}$, $k = 1, \dots, \omega$, can be approximated by the value $f(\theta_{\sigma(j),n})$, σ proper permutation, with an error bounded by $K_f h$, where K_f is a constant depending on f, but independent of h and j (see other works[7–10] and references therein).

The following notation is used throughout this paper. Given a positive integer n and the grid points $\theta_{j,n} = \frac{j\pi}{n+1}$, $j = 1, \dots, n$, the full grid is denoted by the following:

$$\theta_n = \{\theta_{j,n} : j = 1, \dots, n\}.$$

In the same manner, the new gridding defined in Section 2 is denoted by $\tilde{\theta}_n$. When adding a third subscript r, we mean the r:th repetition of j:th grid point, that is, $\tilde{\theta}_{r,j,n}$ is the same for all r with fixed j and n. More specifically, we will use grids of the following form:

$$\tilde{\theta}_n^{(s)} = \left\{\tilde{\theta}_{r,j,n} : \tilde{\theta}_{r,j,n} = \tilde{\theta}_{j,n},\ r = 1, \dots, n/\alpha_s, j = 1, \dots, \alpha_s\right\},$$

such that α_s divides n and $s = 1, 2$. By $\lambda_n, \mu_n, \nu_n, \xi_n$, we denote the ordered sets of eigenvalues in nondecreasing order, of the unsorted eigenvalues using the new grid, of the unsorted eigenvalue approximations from the standard grid and the standard symbol, and of the related approximations in nondecreasing order, respectively.

Here, taking into account the notation above, we furnish more precise estimates in some cases and discuss the general setting, as explained in the following.

More specifically, in Section 2, we consider the special case where $a_0, a_\omega, a_{-\omega} \in \mathbb{C}$, $a_k = 0$ for $k \neq 0, \pm\omega$ (the nontrivial setting is when $a_\omega a_{-\omega} \neq 0$). Under such assumptions, starting from the generating function $f(\theta) = a_0 + a_\omega e^{\mathbf{i}\omega\theta} + a_{-\omega} e^{-\mathbf{i}\omega\theta}$ and from the grid $\tilde{\theta}_n = \{\tilde{\theta}_{j,n} : j = 1, \dots, n\}$ described in Section 2.1, we give the closed form expression of the eigenvalues and eigenvectors in Section 2.2: a new simplified symbol emerges because the eigenvalues $\mu_n = \{\mu_{j,n}\}$, where $j = 1, \dots, n$, are exactly given as $\mu_{j,n} = g\left(\tilde{\theta}_{j,n}\right)$, with $\tilde{\theta}_n$, a proper grid, on $[0, \pi]$ and $g(\theta) = a_0 + 2\sqrt{a_\omega a_{-\omega}}\cos(\theta)$, where the new symbol $g(\theta)$ is different from the generating function $f(\theta) = a_0 + a_\omega e^{\mathbf{i}\omega\theta} + a_{-\omega} e^{-\mathbf{i}\omega\theta}$ and does not depend on ω, whereas the grid $\tilde{\theta}_n$ contains the information on ω. Finally, in Section 2.3, we discuss few relationships between the symbol g and the generating function f, in terms of the concepts of rearrangement (see, for example, other works[11] and references therein) and of spectral symbol in the Weyl sense.

In Section 3, we impose real symmetry to the matrices (1) and consider different cases. More in detail in Section 3.1, we assume that the only nonzero real coefficients of (1) are a_0 and $a_\omega = a_{-\omega}$. We compare the true eigenvalues $\lambda_{j,n}$, $j = 1, \dots, n$, sorted in a nondecreasing order, with the generating function $f(\theta) = a_0 + 2a_\omega \cos(\omega\theta)$ evaluated at the grid given by the points $\frac{j\pi}{n+1}$, which does not lead to an exact representation (except for $\omega = 1$). A closed form symbol and grid for the exact evaluation of the eigenvalues are reported in Theorem 1, and in comparison with the given representation, the accuracy of the algorithm in the work of Ekström et al.[9] is examined.

For any given sequence of indices n, where $\beta = \mathrm{mod}(n, \omega)$, $\beta = 0, 1, \dots, \omega - 1$, we show numerically that ω different "error modes" emerge, and hence, in total, ω^2 different "error modes" can be observed for a symbol of the type $f(\theta) = a_0 + 2a_\omega \cos(\omega\theta)$.

We show that each error mode $s = 0, \dots, \omega - 1$, of a given β, has the following form:

$$E^{\{s\}}_{j_\omega, n_\omega + \eta} = \lambda_{j_s,n} - f\left(\theta_{\sigma_n(j_s),n}\right) = \sum_{k=1}^{\infty} c_{k,s}\left(\theta_{\sigma_n(j_s),n}\right) h^k, \qquad h = \frac{1}{n+1}$$

and present analytical and numerical results regarding $c_{k,s}(\theta)$; see (45) and (46) for the formal definition of all variables.

On the other hand, when considering the finite-difference approximation of the operators $(-1)^q \frac{\partial^{2q}}{\partial x^{2q}}$, $q \geq 1$,we obtain Toeplitz matrices $T_n(f)$ with $f(\theta) = (2 - 2\cos(\theta))^q$ (the case of $q = 1$ coincides with $a_0 = 2$, $a_\omega = a_{-\omega} = -1$, $\omega = 1$). In such a case with $q > 1$, and more generally for monotone symbols f, the error below has the following form:

$$E_{j,n} = \lambda_{j,n} - f\left(\theta_{j,n}\right) = \sum_{k=1}^{\infty} c_k\left(\theta_{j,n}\right) h^k, \qquad h = \frac{1}{n+1}, \tag{3}$$

with $\theta_{j,n} = j\pi h, j = 1, \dots, n$, and $c_k(\theta)$, $k = 1, 2, \dots$, higher order symbols (regarding (3), see the algorithmic proposals and related numerics in the work of Ekström et al.,[9] the analysis in the work of Bogoya et al.,[12] and extensions to preconditioned and differential problems in other works[13,14]).

The functions $c_{k,s}(\theta)$ and $c_k(\theta)$ can be approximated, and a scheme is presented for performing such computations. When f is a cosine trigonometric polynomial monotone on $[0, \pi]$, it is worthwhile to mention that in other works,[15,16] expansions as in (3) are in part formally proven: however, one of the assumptions, that is, the positivity of the second derivative at zero (see page 310, line 3, in the work of Bogoya et al.[15]), excludes the important case of finite-difference approximations of (high-order) differential operators considered because $f(\theta) = (2 - 2\cos(\theta))^q$. However, even if some of the functions c_k can become discontinuous in this setting, as shown in the work of Ekström et al.,[9] the given expansions can be exploited for designing fast eigensolvers also for large matrix sizes.

In Section 3.2, we analyze the case of the general matrices in (1) with a_k being real, $a_k = a_{-k}$, $k = 1, \dots, \omega$. We consider the features and behavior of the error of the eigenvalue approximation using the symbol, because in this setting, a grid and a function giving the exact eigenvalues are not known. However, we show numerically that the eigenvalue behavior of a general banded symmetric Toeplitz matrix with real entries can be described, qualitatively in terms of the symmetrically sparse tridiagonal case with real a_0, $a_\omega = a_{-\omega}$, $\omega = 2, 3, \dots$, and also quantitatively in terms of those having monotone symbols as those related to the classical finite-difference discretization of the operators $(-1)^q \frac{\partial^{2q}}{\partial x^{2q}}$, $q \in \mathbb{N}$, $q \neq 0, 1$.

Some conclusions and possible directions for extending the current results are given in Section 4.

2 | EXACT EIGENVALUES AND EIGENVECTORS OF SYMMETRICALLY SPARSE TRIDIAGONAL, COMPLEX-VALUED TOEPLITZ MATRICES AND THE RELATED SYMBOLS

Let A_n be a Toeplitz matrix of order n and with the following nonzero structure:

$$A_n = \begin{bmatrix} a_0 & \overbrace{0 & \cdots & 0}^{\omega-1} & a_{-\omega} & & \\ 0 & a_0 & \ddots & \ddots & \ddots & \ddots & \\ \vdots & \ddots & \ddots & \ddots & \ddots & \ddots & a_{-\omega} \\ 0 & \ddots & \ddots & \ddots & \ddots & \ddots & 0 \\ a_\omega & \ddots & \ddots & \ddots & \ddots & \ddots & \vdots \\ & \ddots & \ddots & \ddots & \ddots & a_0 & 0 \\ & & a_\omega & 0 & \cdots & 0 & a_0 \end{bmatrix}, \tag{4}$$

and let the constant coefficients $a_0, a_\omega, a_{-\omega}$ be either real or complex. The constants a_ω and $a_{-\omega}$ are located on the $\omega, -\omega$ off-diagonals, respectively. The standard generating function of the matrix $A_n = T_n(f)$ is defined as follows:

$$f(\theta) = a_0 + a_\omega e^{\mathbf{i}\omega\theta} + a_{-\omega} e^{-\mathbf{i}\omega\theta}, \tag{5}$$

which is also the symbol of the sequence of matrices $\{A_n = T_n(f)\}$ in the Weyl sense.[1,3–5] Notably, when $a_\omega a_{-\omega} \neq 0$, the matrix A_n can be symmetrized in the sense that there exists a diagonal invertible matrix D_n such that

$$A_n^{\text{sym}} = D_n A_n D_n^{-1} = \begin{bmatrix} a_0 & \overbrace{0 & \cdots & 0}^{\omega-1} & \sqrt{a_\omega a_{-\omega}} & & \\ 0 & a_0 & \ddots & \ddots & \ddots & \ddots & \\ \vdots & \ddots & \ddots & \ddots & \ddots & \ddots & \sqrt{a_\omega a_{-\omega}} \\ 0 & \ddots & \ddots & \ddots & \ddots & \ddots & 0 \\ \sqrt{a_\omega a_{-\omega}} & \ddots & \ddots & \ddots & \ddots & \ddots & \vdots \\ & \ddots & \ddots & \ddots & \ddots & a_0 & 0 \\ & & \sqrt{a_\omega a_{-\omega}} & 0 & \cdots & 0 & a_0 \end{bmatrix}. \tag{6}$$

Therefore, A_n and A_n^{sym} are similar and share the same eigenvalues, where $A_n^{sym} = T_n(g_\omega)$ with

$$g_\omega(\theta) = a_0 + 2\sqrt{a_\omega a_{-\omega}}\cos(\omega\theta). \tag{7}$$

For the particular case $\omega = 1$, by defining the equidistant grid as follows:

$$\theta_{j,n} = \frac{j\pi}{n+1} = j\pi h, \quad j = 1, \ldots, n, \quad h = \frac{1}{n+1}, \tag{8}$$

the jth eigenvalue $\mu_{j,n}$[7,17–21] of A_n is known in closed form and is expressed as follows:

$$\mu_{j,n} = a_0 + 2\sqrt{a_\omega a_{-\omega}}\cos\left(\theta_{j,n}\right), \quad j = 1, \ldots, n. \tag{9}$$

We notice that $\mu_{j,n} = g(\theta_{j,n})$ with $g(\theta) = g_1(\theta) = a_0 + 2\sqrt{a_1 a_{-1}}\cos(\theta)$, for g_ω with $\omega = 1$ given in Equation (7). Furthermore, for the eigenvalue $\mu_{j,n}$, a corresponding eigenvector $\mathbf{x}_{j,n} = [x_1^{(j,n)}, \ldots, x_n^{(j,n)}]^{\mathrm{T}}$ has components given as follows:

$$x_k^{(j,n)} = \left(\sqrt{\frac{a_\omega}{a_{-\omega}}}\right)^k \sin\left(k\theta_{j,n}\right), \quad k = 1, \ldots, n. \tag{10}$$

It is worth noticing that the operations of square root mentioned above and used in the rest of the paper have to be handled carefully: when we write $\sqrt{\alpha/\beta}$, $\sqrt{\alpha\beta}$, we mean $\sqrt{\rho(\alpha)/\rho(\beta)}e^{\mathbf{i}\frac{\omega(\alpha)-\omega(\beta)}{2}}$, $\sqrt{\rho(\alpha)\rho(\beta)}e^{\mathbf{i}\frac{\omega(\alpha)+\omega(\beta)}{2}}$, respectively, with $\gamma = \rho(\gamma)e^{\mathbf{i}\omega(\gamma)}$, $\gamma \in \{\alpha, \beta\}$, $\rho(\gamma) \geq 0$, $\omega(\gamma) \in [0, 2\pi)$. In this way, for instance, $\sqrt{(-1)(-1)} = -1$ and, for example, without this formal convention, the formulae derived from Theorem 2.4 in the book by Böttcher et al.,[17] for the association eigenvalue–eigenvector, are simply false.

We introduce now a new sampling grid, $\tilde{\theta}_n$, which gives the exact eigenvalues $\mu_{j,n}$ for any $a_0, a_\omega, a_{-\omega} \in \mathbb{C}$ and $\omega \in \mathbb{N}, \omega < n$, in (9), and we introduce a modified version of (10) for expressing the corresponding eigenvectors $\mathbf{x}_{j,n}, j = 1, \ldots, n$.

2.1 | The new sampling grid

We start by introducing a new grid $\tilde{\theta}_n$, defined in the subsequent scheme. We first define β as the remainder of the Euclidean division of n by ω, that is,

$$\beta = n - \omega n_\omega, \quad n_\omega = \frac{n-\beta}{\omega}, \quad 0 \leq \beta < n, \quad n, \omega, \beta, n_\omega \in \mathbb{N}, \tag{11}$$

or in other words, β is the modulus operator applied to the pair (n, ω), $\beta = \mathrm{mod}(n, \omega)$, and n_ω is the quotient, which will be used as a "new" n in the subsequent definition of the new grid. We construct two separate grids, each with a standard equidistant sampling, expressed as follows:

$$\theta_{j_1,n_\omega} = \frac{j_1\pi}{n_\omega+1}, \quad j_1 = 1, \ldots, n_\omega, \tag{12}$$

$$\theta_{j_2,n_\omega+1} = \frac{j_2\pi}{n_\omega+2}, \quad j_2 = 1, \ldots, n_\omega+1. \tag{13}$$

We know that there might be multiple eigenvalues of multiplicity greater than one, and thus, we might need to repeat the same grid point several times. More specifically, we set the following gridpoints:

$$\tilde{\theta}^{(1)}_{r_1,j_1,n_\omega(\omega-\beta)} = \theta_{j_1,n_\omega}, \qquad r_1 = 1, \ldots, \omega-\beta, \quad j_1 = 1, \ldots, n_\omega, \tag{14}$$

$$\tilde{\theta}^{(2)}_{r_2,j_2,(n_\omega+1)\beta} = \theta_{j_2,n_\omega+1}, \qquad r_2 = 1, \ldots, \beta, \quad j_2 = 1, \ldots, n_\omega+1, \tag{15}$$

which is the same as writing that the grid points in (12) are repeated $\omega - \beta$ times and the grid points in (13) are repeated β times. Now, define the following two grids:

$$\tilde{\theta}^{(1)}_{n_\omega(\omega-\beta)} = \left\{ \left\{ \tilde{\theta}^{(1)}_{r_1,j_1,n_\omega(\omega-\beta)} \right\}_{r_1=1}^{\omega-\beta} \right\}_{j_1=1}^{n_\omega}, \tag{16}$$

$$\tilde{\theta}^{(2)}_{(n_\omega+1)\beta} = \left\{ \left\{ \tilde{\theta}^{(2)}_{r_2,j_2,(n_\omega+1)\beta} \right\}_{r_2=1}^{\beta} \right\}_{j_2=1}^{n_\omega+1}. \tag{17}$$

The full sampling grid $\tilde{\theta}_n$ is finally given by the union of the two grids (16) and (17), that is,

$$\tilde{\theta}_n = \tilde{\theta}^{(1)}_{n_\omega(\omega-\beta)} \bigcup \tilde{\theta}^{(2)}_{(n_\omega+1)\beta}. \tag{18}$$

For examples of concrete constructions of these grids, refer to the work of Ekström et al.[22]

2.2 | Eigenvalues and eigenvectors described by the new sampling grid

We start with the main results regarding symmetrically sparse tridiagonal (SST) Toeplitz matrices.

Theorem 1. *The eigenvalues of a SST Toeplitz matrix with center diagonal a_0 and two off-diagonals a_ω and $a_{-\omega}$ at off-diagonal $-\omega$ and ω, as in (4), are given by the following:*

$$\mu_{j,n} = g\left(\tilde{\theta}_{j,n}\right) = a_0 + 2\sqrt{a_\omega a_{-\omega}}\cos\left(\tilde{\theta}_{j,n}\right), \quad j = 1, \dots, n, \tag{19}$$

where $\tilde{\theta}_{j,n}$ is the jth component of the grid $\tilde{\theta}_n$ defined in (18).

Remark 1. By $\mu_n^{(1)}$ and $\mu_n^{(2)}$, we denote the set of eigenvalues given by the symbol evaluations of grids $\tilde{\theta}^{(1)}_{n_\omega(\omega-\beta)}$ and $\tilde{\theta}^{(2)}_{(n_\omega+1)\beta}$ given in (16) and (17), respectively. Assume $a_\omega a_{-\omega} \geq 0$, so that $g(\cdot)$ is real valued; let $\lambda_{j,n}$ be the eigenvalues $\mu_{j,n}$ in Theorem 1 sorted in a nondecreasing order, and let π_n be a permutation of $\{1, \dots, n\}$, which sorts the samples $g(\tilde{\theta}_{1,n}), \dots, g(\tilde{\theta}_{n,n})$ in nondecreasing order, that is, $g(\tilde{\theta}_{\pi_n(1),n}) \leq \cdots \leq g(\tilde{\theta}_{\pi_n(n),n})$. Then,

$$\lambda_{j,n} = g\left(\tilde{\theta}_{\pi_n(j),n}\right) \quad j = 1, \dots, n.$$

Theorem 2. *Given a SST Toeplitz matrix with center diagonal a_0 and two off-diagonals a_ω and $a_{-\omega}$ at off-diagonal $-\omega$ and ω, as in (4), the following statements concerning its eigenvalues and eigenvectors hold.*

For each eigenvalue given by $\mu^{(1)}_{r_1,j_1,n_\omega(\omega-\beta)} = g\left(\tilde{\theta}^{(1)}_{r_1,j_1,n_\omega(\omega-\beta)}\right) = g(\theta_{j_1,n_\omega})$ with $j_1 = 1, \dots, n_\omega$, and $r_1 = 1, \dots, \omega-\beta$, we define a corresponding eigenvector $\mathbf{x}^{(1)}_{r_1,j_1,n} = \left[x_1^{(r_1,j_1,n)}, \cdots, x_n^{(r_1,j_1,n)}\right]^{\mathrm{T}}$, with the following components:

$$x^{(r_1,j_1,n)}_{\omega(k_1-1)+r_1+\beta} = \left(\sqrt{\frac{a_\omega}{a_{-\omega}}}\right)^{k_1}\sin\left(k_1\theta_{j_1,n_\omega}\right), \quad k_1 = 1, \dots, n_\omega, \tag{20}$$

and all nondefined components of $\mathbf{x}_{r_1,j_1,n}$ equal to zero.

For each eigenvalue $\mu^{(2)}_{r_2,j_2,(n_\omega+1)\beta} = g\left(\tilde{\theta}^{(2)}_{r_2,j_2,(n_\omega+1)\beta}\right) = g(\theta_{j_2,n_\omega+1})$ with $j_2 = 1, \dots, n_\omega+1$, and $r_2 = 1, \dots, \beta$, we can define a corresponding eigenvector $\mathbf{x}^{(2)}_{r_2,j_2,n} = \left[x_1^{(r_2,j_2,n)}, \dots, x_n^{(r_2,j_2,n)}\right]^{\mathrm{T}}$, where the components are as follows:

$$x^{(r_2,j_2,n)}_{\omega(k_2-1)+r_2} = \left(\sqrt{\frac{a_\omega}{a_{-\omega}}}\right)^{k_2}\sin\left(k_2\theta_{j_2,n_\omega+1}\right), \quad k_2 = 1, \cdots, n_\omega+1, \tag{21}$$

and all nondefined components of $\mathbf{x}_{r_2,j_2,n}$ are equal to zero.

Remark 2. To save memory and evaluations, taking into account (12) and (13), the steps to construct $\tilde{\theta}_n$ can be skipped, as long as the information concerning multiple eigenvalues is stored. Note that if a grid is desired with all $\theta \in \tilde{\theta}_n$ unique in $[0, \pi]$, one can modify the set $\tilde{\theta}_n$ in (18) as follows: take $\theta \in \tilde{\theta}_n/\omega$ and then shift each grid point by appropriate multiples of π/ω. Then, also the symbol reported in Theorem 1 has to be modified, and instead of $g(\theta) = g_1(\theta)$, we use the generating function of the symmetrized matrix A_n^{sym}, that is, $g_\omega(\theta) = a_0 + 2\sqrt{a_\omega a_{-\omega}}\cos(\omega\theta)$.

Proof of Theorem 1 and Theorem 2. The proof for $\omega > 1$ follows the same ideas as for the case $\omega = 1$ presented in the work of Böttcher et al.[17] We start by observing that the matrix A_n in (4) has the standard symbol as follows:

$$f(\theta) = a_0 + a_\omega e^{\mathbf{i}\omega\theta} + a_{-\omega}e^{-\mathbf{i}\omega\theta}.$$

By assuming $a_\omega \neq 0$ and $a_{-\omega} \neq 0$, and defining $\gamma = \sqrt{a_{-\omega}/a_\omega}$, we consider the matrix B_n defined as follows:

$$B_n = \begin{bmatrix} 0 & \overbrace{0 & \cdots & 0}^{\omega-1} & \gamma^2 & & \\ 0 & 0 & \ddots & \ddots & \ddots & \ddots & \\ \vdots & \ddots & \ddots & \ddots & \ddots & \ddots & \gamma^2 \\ 0 & \ddots & \ddots & \ddots & \ddots & \ddots & 0 \\ 1 & \ddots & \ddots & \ddots & \ddots & \ddots & \vdots \\ & \ddots & \ddots & \ddots & \ddots & 0 & 0 \\ & & 1 & 0 & \cdots & 0 & 0 \end{bmatrix}.$$

Thus, B_n has the following symbol:

$$f_B(\theta) = e^{\mathbf{i}\omega\theta} + \gamma^2 e^{-\mathbf{i}\omega\theta} = e^{\mathbf{i}\omega\theta} + \frac{a_{-\omega}}{a_\omega} e^{-\mathbf{i}\omega\theta}.$$

Following the general framework, because $f(\theta) = a_0 + a_\omega f_B(\theta)$, it is sufficient to show that B_n has the eigenvalues as follows:

$$\mu^{(1)}_{r_1,j_1,n_\omega(\omega-\beta)} = 2\gamma\cos\left(\theta_{j_1,n_\omega}\right), \qquad r_1 = 1,\ \dots,\omega-\beta, \quad j_1 = 1,\ \dots,n_\omega, \tag{22}$$

$$\mu^{(2)}_{r_2,j_2,(n_\omega+1)\beta} = 2\gamma\cos\left(\theta_{j_2,n_\omega+1}\right), \qquad r_2 = 1,\ \dots,\beta, \quad j_2 = 1,\cdots,n_\omega+1, \tag{23}$$

and that the following corresponding eigenvectors:

$$\mathbf{x}^{(1)}_{r_1,j_1,n} = \left[x_1^{(r_1,j_1,n)},\cdots,x_n^{(r_1,j_1,n)}\right]^{\mathrm{T}}, \tag{24}$$

$$\mathbf{x}^{(2)}_{r_2,j_2,n} = \left[x_1^{(r_2,j_2,n)},\ \dots,x_n^{(r_2,j_2,n)}\right]^{\mathrm{T}}, \tag{25}$$

have components of the following form:

$$x^{(r_1,j_1,n)}_{\omega(k_1-1)+r_1+\beta} = \gamma^{-k_1}\sin\left(k_1\theta_{j_1,n_\omega}\right), \qquad k_1 = 1,\ \dots,n_\omega, \tag{26}$$

$$x^{(r_2,j_2,n)}_{\omega(k_2-1)+r_2} = \gamma^{-k_2}\sin\left(k_2\theta_{j_2,n_\omega+1}\right), \qquad k_2 = 1,\cdots,n_\omega+1, \tag{27}$$

respectively. Because $B_n\mathbf{x} = \mu\mathbf{x}$ for a given eigenpair $(\mu,\mathbf{x})$, for all k relationships, (28)–(32) must hold true. For $\omega \le n/2$,

$$\gamma^2 x_{\omega+k} = \mu x_k, \qquad k = 1,\ \dots,\omega, \tag{28}$$

$$x_k + \gamma^2 x_{2\omega+k} = \mu x_{\omega+k}, \qquad k = 1,\ \dots,n-2\omega, \tag{29}$$

$$x_{n+1-(\omega+k)} = \mu x_{n+1-k}, \qquad k = 1,\ \dots,\omega. \tag{30}$$

For $n/2 < \omega < n$,

$$\gamma^2 x_{\omega+k} = \mu x_k, \qquad k = 1,\ \dots,n-\omega, \tag{31}$$

$$x_{n+1-(\omega+k)} = \mu x_{n+1-k}, \qquad k = 1,\ \dots,n-\omega. \tag{32}$$

First, we show that Equations (28) and (31) are satisfied. For $\mathbf{x}^{(1)}_{r_1,j_1,n}$ in (24), the nonzero components have indices of the form $\omega(k_1-1)+r_1+\beta$, $k_1 = 1,\ \dots,n_\omega$ (as seen in (26)). For $k_1 = 1$, we have $r_1+\beta$, and for $k_2 = 2$, we have $\omega+r_1+\beta$, which are the only two nonzero components that match (28) and (31). More specifically, we observe the following:

$$x^{(r_1,j_1,n)}_{\omega+r_1+\beta} = \mu^{(1)}_{r_1,j_1,n_\omega(\omega-\beta)} x^{(r_1,j_1,n)}_{r_1+\beta}, \tag{33}$$

or, explicitly,

$$\gamma^2\gamma^{-2}\sin\left(2\theta_{j_1,n_\omega}\right) = 2\gamma\cos\left(\theta_{j_1,n_\omega}\right)\gamma^{-1}\sin\left(\theta_{j_1,n_\omega}\right), \tag{34}$$

that is, $\sin\left(2\theta_{j_1,n_\omega}\right) = 2\cos\left(\theta_{j_1,n_\omega}\right)\sin\left(\theta_{j_1,n_\omega}\right)$, which is true, owing to the trigonometric identity as follows:

$$\sin(2\gamma_1) = 2\cos(\gamma_1)\sin(\gamma_1). \tag{35}$$

For $\mathbf{x}^{(2)}_{r_2,j_2,n}$ in (25), we observe the same behavior as for $\mathbf{x}^{(1)}_{r_1,j_1,n}$ in (24) above, but the relation analogous to (33) is now as follows:

$$x^{(r_2,j_2,n)}_{\omega+r_2} = \mu^{(2)}_{r_2,j_2,(n_\omega+1)\beta} x^{(r_2,j_2,n)}_{r_2}.$$

Namely, it is the same as (34), except for the fact that $\theta_{j_2,n_\omega+1}$ replaces θ_{j_1,n_ω}.

Secondly, we show that (29) is true. For $\mathbf{x}^{(1)}_{r_1,j_1,n}$ in (24), the nonzero components have indices of the form $\omega(k_1-1)+r_1+\beta$, $k_1 = 1,\ \dots,n_\omega$ (as seen in (26)). For k_1, k_1+1, k_1+2, with $k_1 = 1,\ \dots,k^{r_1,j_1}_{\max}$, where $k^{r_1,j_1}_{\max} \le (n-r_1-\beta-\omega)/\omega$, $k^{r_1,j_1}_{\max} \in \mathbb{N}$, we find all nonzero terms of (29) expressed as follows:

$$x^{(r_1,j_1,n)}_{\omega(k_1-1)+r_1+\beta} + \gamma^2 x^{(r_1,j_1,n)}_{\omega(k_1+1)+r_1+\beta} = \mu^{(1)}_{r_1,j_1,n_\omega(\omega-\beta)} x^{(r_1,j_1,n)}_{\omega k_1+r_1+\beta}.$$

Explicitly, we deduce the following:

$$\gamma^{-(\omega(k_1-1)+r_1+\beta)}\sin\left((\omega(k_1-1)+r_1+\beta)\,\theta_{j_1,n_\omega}\right)$$
$$+\gamma^2\gamma^{-(\omega(k_1+1)+r_1+\beta)}\sin\left((\omega(k_1+1)+r_1+\beta)\,\theta_{j_1,n_\omega}\right)=2\gamma\cos\left(\theta_{j_1,n_\omega}\right)\gamma^{-(\omega k_1+r_1+\beta)}\sin\left((\omega k_1+r_1+\beta)\,\theta_{j_1,n_\omega}\right),$$

or

$$\sin\left((\omega(k_1-1)+r_1+\beta)\,\theta_{j_1,n_\omega}\right)+\sin\left((\omega(k_1+1)+r_1+\beta)\,\theta_{j_1,n_\omega}\right)=2\cos\left(\theta_{j_1,n_\omega}\right)\sin\left((\omega k_1+r_1+\beta)\,\theta_{j_1,n_\omega}\right),$$

which is satisfied because of the trigonometric identity as follows:

$$\sin(\gamma_1)+\sin(\gamma_2)=2\cos\left(\frac{\gamma_1-\gamma_2}{2}\right)\sin\left(\frac{\gamma_1+\gamma_2}{2}\right).$$

For $\mathbf{x}^{(2)}_{r_2,j_2,n}$ in (25), for $k_2=1,\cdots,k^{r_2,j_2}_{\max}$, where $k^{r_2,j_2}_{\max}\le(n-r_2-\omega)/\omega, k^{r_2,j_2}_{\max}\in\mathbb{N}$, taking into account (29), we find the following:

$$x^{(r_2,j_2,n)}_{\omega(k_2-1)+r_2}+\gamma^2x^{(r_2,j_2,n)}_{\omega(k_2+1)+r_1}=\mu^{(2)}_{r_2,j_2,(n_\omega+1)\beta}x^{(r_2,j_2,n)}_{\omega k_2+r_2},$$

and this is proven for the case $\mu^{(1)}_{r_1,j_1,n_\omega(\omega-\beta)}$ and $\mathbf{x}^{(1)}_{r_1,j_1,n}$ described above.

As last step, we show that the relationships in (30) and (32) are true. For $\mathbf{x}^{(1)}_{r_1,j_1,n}$ in (24), the nonzero components have indices of the form $\omega(k_1-1)+r_1+\beta, k_1=1,\ldots,n_\omega$ (as seen in (26)). For $k_1=n_\omega$, we find $n+r_1-\omega$, and for $k_2=n_\omega-1$, we have $n+r_1-2\omega$, which are the only two nonzero components that match (30) and (32), namely,

$$x^{(r_1,j_1,n)}_{n+r_1-2\omega}=\mu^{(1)}_{r_1,j_1,n_\omega(\omega-\beta)}x^{(r_1,j_1,n)}_{n+r_1-\omega}. \tag{36}$$

More in detail, we infer that

$$\begin{aligned}\gamma^{-(n_\omega-1)}\sin\left((n_\omega-1)\theta_{j_1,n_\omega}\right)&=2\gamma\cos\left(\theta_{j_1,n_\omega}\right)\gamma^{-n_\omega}\sin\left(n_\omega\theta_{j_1,n_\omega}\right),\\ \sin\left((n_\omega-1)\theta_{j_1,n_\omega}\right)&=2\cos\left(\theta_{j_1,n_\omega}\right)\sin\left(n_\omega\theta_{j_1,n_\omega}\right),\\ \sin\left((n_\omega-1)\frac{j_1\pi}{n_\omega+1}\right)&=2\cos\left(\frac{j_1\pi}{n_\omega+1}\right)\sin\left(n_\omega\frac{j_1\pi}{n_\omega+1}\right).\end{aligned} \tag{37}$$

Furthermore, because

$$\begin{aligned}\sin\left((n_\omega-1)\frac{j_1\pi}{n_\omega+1}\right)&=\sin\left(j_1\pi-2\frac{j_1\pi}{n_\omega+1}\right)=(-1)^{j_1+1}\sin\left(2\frac{j_1\pi}{n_\omega+1}\right),\\ \sin\left(n_\omega\frac{j_1\pi}{n_\omega+1}\right)&=\sin\left(j_1\pi-\frac{j_1\pi}{n_\omega+1}\right)=(-1)^{j_1+1}\sin\left(\frac{j_1\pi}{n_\omega+1}\right),\end{aligned}$$

we deduce that relation (37) is equivalent to $\sin\left(2\theta_{j_1,n_\omega}\right)=2\cos\left(\theta_{j_1,n_\omega}\right)\sin\left(\theta_{j_1,n_\omega}\right)$, which is an identity, because of the basic relation in (35). Equivalently, the latter is true for $\mu^{(2)}_{r_2,j_2,(n_\omega+1)\beta}$ in (23) and for $\mathbf{x}^{(2)}_{r_2,j_2,n}$ in (25). □

2.3 | The real symmetric SST Toeplitz case: the generating function and a simplified distribution function

We now consider the previous results from the point of view of spectral distributions in the sense of Weyl. First, we introduce some notations and definitions concerning the general sequences of matrices. For any function F defined on the complex field and for any matrix A_n of size d_n, by the symbol $\Sigma_\lambda(F,A_n)$, we denote the following means:

$$\frac{1}{d_n}\sum_{j=1}^{d_n}F\left[\lambda_j(A_n)\right].$$

Moreover, given a sequence $\{A_n\}$ of matrices of size d_n with $d_n<d_{n+1}$ and given a Lebesgue-measurable function ψ defined over a measurable set $K\subset\mathbb{R}^\nu$, $\nu\in\mathbb{N}^+$, of finite e positive Lebesgue measure $\mu(K)$, we say that $\{A_n\}$ is distributed as (ψ,K) in the sense of the eigenvalues if for any continuous F with bounded support, the following limit relation holds:

$$\lim_{n\to\infty}\Sigma_\lambda(F,A_n)=\frac{1}{\mu(K)}\int_K F(\psi)\,\mathrm{d}\mu. \tag{38}$$

In this case, we write in short $\{A_n\} \sim_\lambda (\psi, K)$. In Remark 3, we provide an informal meaning of the notion of eigenvalue distribution.

Remark 3. The informal meaning behind the above definition is the following. If ψ is continuous, n is large enough, and

$$\left\{\mathbf{x}_j^{(m_n)}, \quad j = 1, \ldots, d_n\right\}$$

is an equispaced grid on K, then a suitable ordering $\lambda_j(A_n), j = 1, \ldots, d_n$, of the eigenvalues of A_n is such that the pairs $\left\{\left(\mathbf{x}_j^{(d_n)}, \lambda_j(A_n)\right), \quad j = 1, \cdots, m_n\right\}$ reconstruct approximately the hypersurface as follows:

$$\{(\mathbf{x}, \psi(\mathbf{x})), \ \mathbf{x} \in K\}.$$

In other words, the spectrum of A_n "behaves" like a uniform sampling of ψ over K. For instance, if $\nu = 1$, $d_n = n$, and $K = [a, b]$, then the eigenvalues of A_n are approximately equal to $\psi(a + j(b-a)/n), j = 1, \ldots, n$, for n large enough. Analogously, if $\nu = 2$, $d_n = n^2$, and $K = [a_1, b_1] \times [a_2, b_2]$, then the eigenvalues of A_n are approximately equal to $\psi(a_1 + j(b_1 - a_1)/n, a_2 + k(b_2 - a_2)/n), j, k = 1, \ldots, n$, for n large enough.

Let f be a complex-valued (Lebesgue) integrable function, defined over $Q = (-\pi, \pi)$, and let us consider the sequence $\{T_n(f)\}$ with $T_n(f) = \left(\hat{f}_{j-k}\right)_{j,k=1}^n$, $\hat{f}_s, s \in \mathbb{Z}$ being the Fourier coefficients of f defined as in (2). The asymptotic distribution of eigenvalues and singular values of a sequence of Toeplitz matrices has been thoroughly studied in the last century (for example, see other works[1,23] and the references reported therein). The starting point of this theory, which contains many extensions and other results, is a famous theorem of Szegő,[3] which we report in the version given by Tyrtyshnikov et al.[23]

Theorem 3. *If f is integrable over Q, and if $\{T_n(f)\}$ is the sequence of Toeplitz matrices generated by f, it then holds that*

$$\{T_n^*(f)T_n(f)\} \sim_\lambda \left(|f|^2, Q\right). \tag{39}$$

Moreover, if f is also real valued, then each matrix $T_n(f)$ is Hermitian and

$$\{T_n(f)\} \sim_\lambda (f, Q). \tag{40}$$

However, a simple remark has to be added. The symbol in the Weyl sense is far from unique, and in fact, any rearrangement is still a symbol. A simple case is given by standard Toeplitz sequences $\{T_n(f)\}$, with f real valued, and even that is $f(\theta) = f(-\theta)$ almost everywhere, $\theta \in Q$. In that case, relation (40) has the following form:

$$\lim_{n\to\infty} \Sigma_\lambda(F, T_n(f)) = \frac{1}{2\pi}\int_{-\pi}^{\pi} F(f(\theta))\,\mathrm{d}\theta = \frac{1}{\pi}\int_0^{\pi} F(f(\theta))\,\mathrm{d}\theta, \tag{41}$$

due to the even character of f, and hence, $\{T_n(f)\} \sim_\lambda (f, Q_+)$, $Q_+ = (0, \pi)$. In fact, the grid points are not searched in the big interval Q but in the restricted interval Q_+ (see Remark 3).

However, formula (19) in Theorem 1 seems to be confusing, because the generating function is $g_\omega(\theta) = a_0 + 2a_\omega \cos(\omega\theta)$, whereas the eigenvalues result in an equispaced sampling of the function $a_0 + 2|a_\omega| \cos(\theta)$. Because Theorem 3 tells one that $\{T_n(g_\omega)\} \sim_\lambda (g_\omega, Q)$, whereas our explicit computation implies $\{T_n(g_\omega)\} \sim_\lambda (g_1, Q_+)$, it follows that g_1 on Q_+ is a rearrangement of g_ω on Q. Indeed, the latter is true, as demonstrated in the following simple derivations:

$$\begin{aligned}
\int_{-\pi}^{\pi} F(g_\omega(\theta))\,\mathrm{d}\theta &= \int_0^{2\pi} F(g_\omega(\theta))\,\mathrm{d}\theta \\
&= \omega\int_0^{2\pi/\omega} F(g_\omega(\theta))\,\mathrm{d}\theta \\
&= \omega\int_0^{2\pi} F(g_\omega(s/\omega))\,\mathrm{d}s/\omega \\
&= \int_0^{2\pi} F(g_1(s))\,\mathrm{d}s = 2\int_0^{\pi} F(g_1(s))\,\mathrm{d}s.
\end{aligned}$$

By the way, the fact that g_1 has exactly two branches, one monotonically increasing on $(0, \pi/2)$ and the other monotonically decreasing on $(\pi/2, \pi)$, represents a qualitative confirmation of the fact that the grid $\tilde{\theta}_n$ in (18), for the exact eigenvalue formulae, is obtained by the merging of exactly two distinct grids, $\tilde{\theta}^{(1)}_{n_\omega(\omega-\beta)}$ and $\tilde{\theta}^{(2)}_{(n_\omega+1)\beta}$, independently of the parameter ω.

3 | THE REAL SYMMETRIC SST CASE AND ITS USE IN THE GENERAL SYMMETRIC BANDED TOEPLITZ CASE

Let A_n be a Toeplitz matrix of order n and let $\hat{\omega} < n$ be a positive integer as follows:

$$A_n = \begin{bmatrix} a_0 & a_1 & \cdots & a_{\hat{\omega}} & & & & \\ a_1 & a_0 & \ddots & & \ddots & & & \\ \vdots & \ddots & \ddots & \ddots & & \ddots & & \\ a_{\hat{\omega}} & & \ddots & \ddots & \ddots & & \ddots & \\ & \ddots & & \ddots & \ddots & \ddots & & a_{\hat{\omega}} \\ & & \ddots & & \ddots & \ddots & \ddots & \vdots \\ & & & \ddots & & \ddots & a_0 & a_1 \\ & & & & a_{\hat{\omega}} & \cdots & a_1 & a_0 \end{bmatrix}, \tag{42}$$

where the coefficients a_k, $k = 0, \ldots, \hat{\omega}$, are real numbers.

We now show that the behavior of the spectrum of such matrices can be qualitatively described via the spectral behavior of two different types of matrices: matrices of the form in (4) with different $\omega = 2, \ldots, \hat{\omega}$ and with $a_0, a_\omega = a_{-\omega}$, real numbers, and matrices of the form (42) with monotone generating function f on $[0, \pi]$, as the case of $f(\theta) = (2 - 2\cos(\theta))^2$. We observe that the case $f(\theta) = (2 - 2\cos(\theta))^2$ corresponds to the choice of $q = 2$ with $a_0 = 6, a_1 = -4, a_2 = 1$ and that for such a case, an expansion similar to that in (3) holds. We remind that expansions as in (3) are observed in other works[9,15] (and formally proven under mild assumptions[15]) for the general case, in which the generating function is a monotone cosine polynomial in $[0, \pi]$.

In Section 3.1, we compare the generating function $g_\omega(\theta) = 2 - 2\cos(\omega\theta)$ with the spectrum of matrices of the form in (4) with different $\omega = 2, \ldots, q$ and with $a_0, a_\omega = a_{-\omega}$, real numbers, by proving the expansions in (44).

In Section 3.2, for a general matrix of the form (42), we show numerical evidences that a qualitative comparison between the eigenvalues and the generating function is described either by an expansion like (3), characterizing the monotone case, or by an expansion like (44), characterizing the purely oscillatory case as $g_\omega(\theta) = 2 - 2\cos(\omega\theta)$, $\omega = 2, \ldots, q$. From a computational viewpoint, as explained by Ekström et al.,[9] the crucial observation is that such a qualitative behavior turns out to be the theoretical key for designing fast extrapolation-type algorithms for computing eigenvalues of large matrices of the form reported in (42).

3.1 | The real symmetric SST Toeplitz case: eigenvalues and generating function

Typically, a correct symbol and grid combination, which together exactly samples the eigenvalues of a given matrix, is not known, but the error can be reconstructed in some cases; see the work of Ekström et al.[9]

When approximating the eigenvalues for the standard nonmonotone symbol as follows:

$$f(\theta) = g_\omega(\theta) = 2 - 2\cos(\omega\theta), \tag{43}$$

with $1 < \omega$ fixed with respect to n, and sampling $g_\omega(\cdot)$ at the standard equispaced grid of (8), we obtain the exact eigenvalues plus an error. This error can be expressed analytically, because the eigenvalues are given by Theorem 1. Subsequently, we furnish an expression for the expansion of such an error (refer also to the work of Ekström et al.[9] for similar expansions in the monotone case).

We begin by defining the permutations $\pi_n, \sigma_n : \{1, \ldots, n\} \to \{1, \ldots, n\}$ such that $g(\tilde{\theta}_{\pi_n(1),n}) \le \cdots \le g(\tilde{\theta}_{\pi_n(n),n})$, $f(\theta_{\sigma_n(1),n}) \le \cdots \le f(\theta_{\sigma_n(n),n})$. We denote $\mu_{j,n} = g(\tilde{\theta}_{j,n})$, $\lambda_{j,n} = g(\tilde{\theta}_{\pi_n(j),n})$, and $\nu_{j,n} = f(\theta_{j,n})$, $\xi_{j,n} = g(\theta_{\sigma_n(j),n})$.

The error for (43) with sampling grid (8) to approximate the eigenvalues after sorting is thus

$$E_{j,n} = g\big(\tilde{\theta}_{\pi_n(j),n}\big) - f\big(\theta_{\sigma_n(j),n}\big) = \lambda_{j,n} - \xi_{j,n}. \tag{44}$$

This error is shown, for example, in Figure 1(a)–(c) in light gray for $\omega = 3$. At first glance, this error can seem chaotic, but it is clear numerically that in this case, and for any $1 < \omega < n$, there will be ω^2 different "error modes"; ω different modes for any fixed $\beta = \mathrm{mod}(n, \omega) \in \{0, \ldots, \omega - 1\}$. Indeed, for each β, we will denote the different error modes by $s = 0, \ldots, \omega - 1$. In Figure 1(a)–(c), these modes are shown for $\beta = 0, 1, 2$, $s = 0$ yellow (dotted), $s = 1$ blue (solid), and $s = 2$ red (dashed). Each error mode for a given n and β is given by the indices $j_s \in I_s, s = 0, \ldots, \omega - 1$, where $I_s = \{s, s + \omega, s + 2\omega, \ldots\}$ (except for $s = 0$ where $I_0 = \{\omega, 2\omega, \ldots\}$), and the union of all I_s is the whole set of indices $\{1, \ldots, n\}$. In other words, $s = \mathrm{mod}(j, \omega)$ for $j = 1, \ldots, n$, and for $s = 0$, we have $j_0 = j_\omega \omega$, $j_\omega = 1, \ldots, n_\omega$ and $s > 0$,

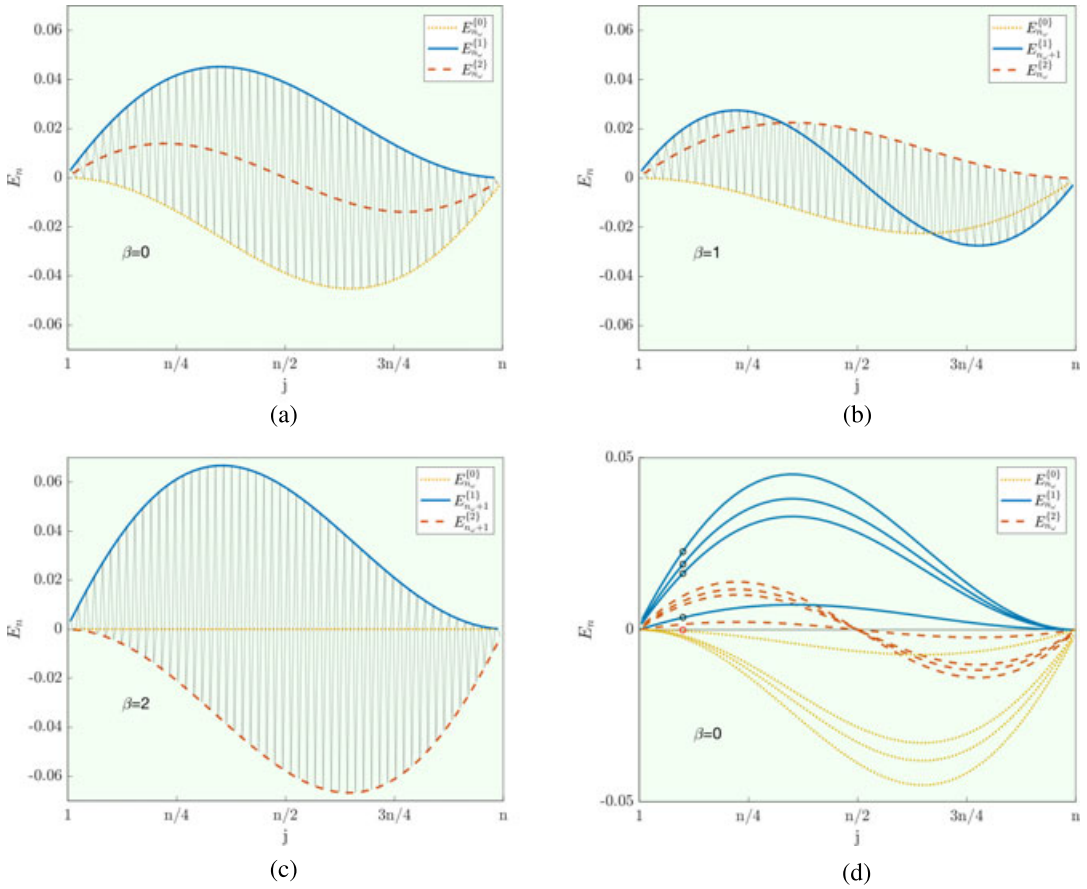

FIGURE 1 Errors for eigenvalue approximations for matrices of different sizes with standard symbol $g_3(\theta) = 2 - 2\cos(3\theta)$ and grids $\theta_{j,n} = j\pi h, j = 1, \dots, n, h = 1/(n+1)$. For each $\beta = \text{mod}(n, \omega) = \text{mod}(n, 3)$, there exist $\omega = 3$ different error modes $E^{\{i\}}_{n_\omega+\eta}, i = 0, 1, 2$, represented in yellow (dotted), blue (solid), and red (dashed). In gray, we show the errors not separated into different error modes. In panel (d), the error reduction for $g_3(\theta) = 2 - 2\cos(3\theta)$ for $\bar{\theta} = \pi/10$ is reported, by using the algorithm presented by Ekström et al.[9] (a) n = 159, $\beta = 0$. (b) n = 160, $\beta = 1$. (c) n = 161, $\beta = 2$. (d) Estimation of $c_{k,0}, k = 1, 2, 3; \bar{\theta} = \pi/10, \beta = 0$

$j_s = s + (j_\omega - 1)\omega, j_\omega = 1, \dots n_\omega + \eta$, where $n_\omega = (n - \beta)/\omega$ and $\eta = 1$ for $s = 1, \dots, \beta$, and otherwise, $\eta = 0$. In this setting, there exist functions $c_{k,s}(\cdot), s = 0, 1, \dots, \omega - 1, k \geq 1$ for which the following error:

$$E_{j_s,n} = g\left(\tilde{\theta}_{\pi_n(j_s),n}\right) - f\left(\theta_{\sigma_n(j_s),n}\right) = \lambda_{j_s,n} - \xi_{j_s,n} = \lambda^{\{s\}}_{j_\omega,n_\omega+\eta} - \xi^{\{s\}}_{j_\omega,n_\omega+\eta} = E^{\{s\}}_{j_\omega,n_\omega+\eta} \tag{45}$$

has the following form:

$$E^{\{s\}}_{j_\omega,n_\omega+\eta} = \sum_{k=1}^{\infty} c_{k,s}\left(\theta_{\sigma_n(j_s),n}\right) h^k, \quad h\frac{1}{n+1}. \tag{46}$$

We will refer to the functions $c_{k,s}(\theta), k = 1, 2, \dots, s = 0, 1, \dots, \omega - 1$ as higher order symbols.

Example 1. As a demonstrative example, we will look at the symbol $f_3(\theta) = 2 - 2\cos(3\theta)$. We have $n = 12$, and because $\omega = 3$, we have $\beta = 0$ and $n_\omega = 4$. Because $\beta = 0$ is the simplest case where $\tilde{\theta}_n = \tilde{\theta}^{(1)}_n$, which consists of $\theta_{n_\omega} = \theta_4$ repeated $\omega - \beta = 3$ times, we have the following:

$$\theta_{j_1,n_\omega} = \frac{j_1\pi}{n_\omega + 1} \quad j_1 = 1, \dots, n_\omega, \quad \theta_{j,n} = \frac{j\pi}{n+1}, \quad j = 1, \dots, n.$$

In the following table, the different evaluations are reported.

j	1	2	3	4	5	6	7	8	9	10	11	12
$f_3(\theta_{j,n}) = \nu_{j,12}$	$\nu_{1,12}$	$\nu_{2,12}$	$\nu_{3,12}$	$\nu_{4,12}$	$\nu_{5,12}$	$\nu_{6,12}$	$\nu_{7,12}$	$\nu_{8,12}$	$\nu_{9,12}$	$\nu_{10,12}$	$\nu_{11,12}$	$\nu_{12,12}$
$g(\tilde{\theta}_{j,n}) = \mu_{j,12}$	$\mu_{1,4}$	$\mu_{1,4}$	$\mu_{1,4}$	$\mu_{2,4}$	$\mu_{2,4}$	$\mu_{2,4}$	$\mu_{3,4}$	$\mu_{3,4}$	$\mu_{3,4}$	$\mu_{4,4}$	$\mu_{4,4}$	$\mu_{4,4}$.

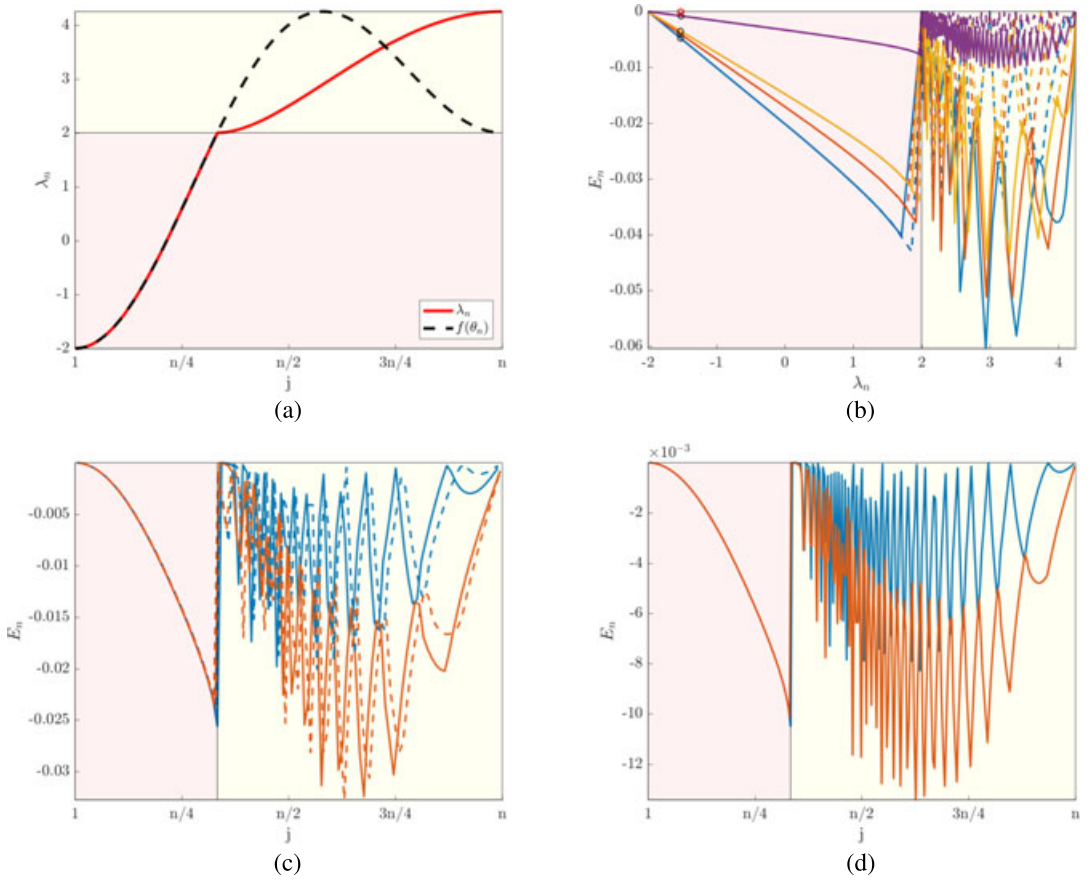

FIGURE 2 Eigenvalues, symbol, and errors for matrices with standard symbol $f(\theta) = 2 - 2\cos(\theta) - 2\cos(2\theta)$ and grids $\theta_{j,n} = j\pi h, j = 1, \ldots, n, h = 1/(n+1)$. (a) True eigenvalues (sorted, solid in red). Sampling of the symbol (unsorted, dashed in black). (b) Errors for different n. Reduction of error for $\bar{\theta} = \pi/10$. (c) Errors for n 200 (solid) and $n = 202$ (dashed). (d) Errors for $n = 500$

Sorting the evaluations of $g(\tilde{\theta}_{j,n})$ in nondecreasing order, that is, $g(\tilde{\theta}_{\pi_n(j),n})$, we will have the true eigenvalues as follows:

$$\lambda_{12} = \left\{\mu_{4,4}, \mu_{4,4}, \mu_{4,4}, \mu_{3,4}, \mu_{3,4}, \mu_{3,4}, \mu_{2,4}, \mu_{2,4}, \mu_{2,4}, \mu_{1,4}, \mu_{1,4}, \mu_{1,4}\right\}.$$

By splitting the eigenvalues by the different indices in order to separate the error modes, we obtain the following:

$$\begin{aligned}
\lambda_4^{\{0\}} &= \left\{\mu_{4,4}, \mu_{3,4}, \mu_{2,4}, \mu_{1,4}\right\} = \left\{\lambda_{j_0,12}\right\}, && j_0 = 3, 6, 9, 12, \quad s = \text{mod}(j_0, \omega) = 0,\\
\lambda_4^{\{1\}} &= \left\{\mu_{4,4}, \mu_{3,4}, \mu_{2,4}, \mu_{1,4}\right\} = \left\{\lambda_{j_1,12}\right\}, && j_1 = 1, 4, 7, 10, \quad s = \text{mod}(j_1, \omega) = 1,\\
\lambda_4^{\{2\}} &= \left\{\mu_{4,4}, \mu_{3,4}, \mu_{2,4}, \mu_{1,4}\right\} = \left\{\lambda_{j_2,12}\right\}, && j_2 = 2, 5, 8, 11, \quad s = \text{mod}(j_2, \omega) = 2.
\end{aligned}$$

Sorting the evaluations of $f(\theta_{j,n})$ in a nondecreasing order, that is, $f(\theta_{\sigma_n(j),n})$, we will have the approximations of the eigenvalues as follows:

$$\xi_{12} = \left\{\nu_{9,12}, \nu_{8,12}, \nu_{1,12}, \nu_{10,12}, \nu_{7,12}, \nu_{2,12}, \nu_{11,12}, \nu_{6,12}, \nu_{3,12}, \nu_{12,12}, \nu_{5,12}, \nu_{4,12}\right\}.$$

By splitting the approximations of the eigenvalues by the different indices for separating the error modes, we find the following:

$$\begin{aligned}
\xi_4^{\{0\}} &= \left\{\nu_{1,12}, \nu_{2,12}, \nu_{3,12}, \nu_{4,12}\right\} = \left\{\xi_{j_0,12}\right\}, && j_0 = 3, 6, 9, 12, \quad s = \text{mod}(j_0, \omega) = 0,\\
\xi_4^{\{1\}} &= \left\{\nu_{9,12}, \nu_{10,12}, \nu_{11,12}, \nu_{12,12}\right\} = \left\{\xi_{j_1,12}\right\}, && j_1 = 1, 4, 7, 10, \quad s = \text{mod}(j_1, \omega) = 1,\\
\xi_4^{\{2\}} &= \left\{\nu_{8,12}, \nu_{7,12}, \nu_{6,12}, \nu_{5,12}\right\} = \left\{\xi_{j_2,12}\right\}, && j_2 = 2, 5, 8, 11, \quad s = \text{mod}(j_2, \omega) = 2.
\end{aligned}$$

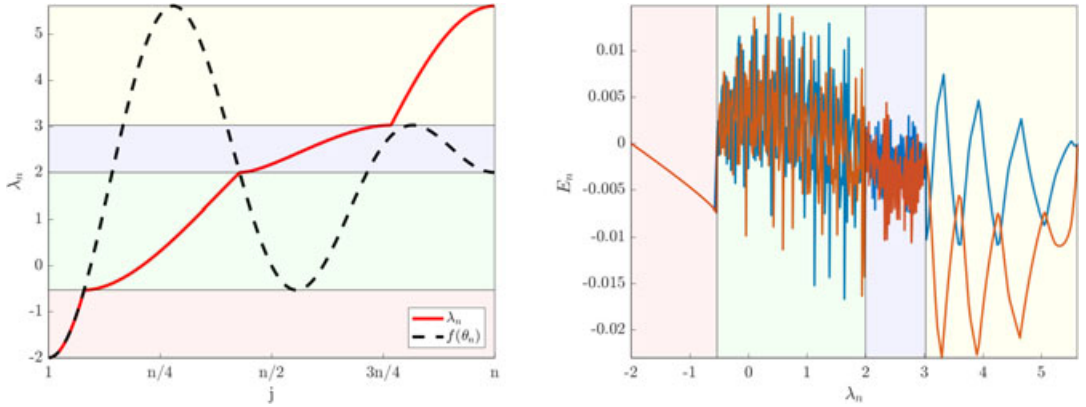

(a) (b)

FIGURE 3 Eigenvalues, symbol, and errors for a matrix with standard symbol $f(\theta) = 2 - 2\cos(3\theta) - 2\cos(4\theta)$ and grids $\theta_{j,n} = j\pi h, j = 1, \dots, n, h = 1/(n+1)$. (a) True eigenvalues (sorted, solid in red). Sampling of the symbol (unsorted, dashed in black). (b) Errors for $n = 1000$

Hence, we have ω different error modes for $\omega = 3$ and $\beta = 0$, which are given by the following:

$$E^{\{0\}}_{j_\omega,n_\omega} = g\big(\theta_{n_\omega+1-j_\omega,n_\omega}\big) - f_3\big(\theta_{j_\omega,n}\big) = g\big(\theta_{5-j_\omega,4}\big) - f_3\big(\theta_{j_\omega,12}\big), \qquad j_\omega = 1, \dots, 4, \tag{47}$$

$$E^{\{1\}}_{j_\omega,n_\omega} = g\big(\theta_{n_\omega+1-j_\omega,n_\omega}\big) - f_3\big(\theta_{j_\omega+2n_\omega,n}\big) = g\big(\theta_{5-j_\omega,4}\big) - f_3\big(\theta_{j_\omega+8,12}\big), \qquad j_\omega = 1, \dots, 4, \tag{48}$$

$$E^{\{2\}}_{j_\omega,n_\omega} = g(\theta_{n_\omega+1-j_\omega,n_\omega}) - f_3(\theta_{2n_\omega+1-j_\omega,n}) = g(\theta_{5-j_\omega,4}) - f_3(\theta_{9-j_\omega,12}), \qquad j_\omega = 1, \dots, 4, \tag{49}$$

because $\eta = 0$ in (46) for all $s = 0, 1, 2$, and because $\beta = 0$. Using the algorithm presented by Ekström et al.,[9] we look at a specific eigenvalue of interest $\bar\theta = \pi/10$. By this, we mean that for a matrix of size n, the index of the eigenvalue of interest, when they are sorted in nondecreasing order, $\bar j$, is found by $\pi/10 = \bar j\pi/(n+1)$. The error is then specifically $E_{\bar j,n} = \lambda_{\bar j,n} - \xi_{\bar j,n}$ or $E^{\{1\}}_{j_\omega,n_\omega}$ because $\beta = 0$ for all n of interest in this example. We look specifically at the pairs $(j_1, n_1) = (16, 159), (j_2, n_2) = (19, 189), (j_3, n_3) = (22, 219)$, and $(j, n) = (100, 999)$, which are presented in Figure 1(d). The light green background indicates that the derivative of the symbol changes sign two times in the region. Other examples of a different number of sign changes are presented in Figures 2 and 3. Because $s = \mathrm{mod}(j, \omega) = 1$, the error will have the following expression:

$$E^{\{1\}}_{j_\omega,n_\omega} = g\big(\theta_{n_\omega+1-j_\omega,n_\omega}\big) - f_3\big(\theta_{j_\omega+2n_\omega,n}\big), \qquad j_\omega = 1, \dots, n_\omega, \tag{50}$$

given by (48). We now look at a specific j_ω, namely $\bar j_\omega = (n_\omega + 7)/10$. Hence, the pairs for each error mode are instead $(\bar j_\omega, n_\omega)$, that is, $(6, 53), (7, 63), (8, 73)$, and $(34, 333)$. Explicitly, we obtain the following:

$$E^{\{1\}}_{\bar j_\omega,n_\omega} = g\big(\theta_{n_\omega+1-\bar j_\omega,n_\omega}\big) - f_3\big(\theta_{\bar j_\omega+2n_\omega,n}\big) = \sum_{k=1}^{\infty} c_{k,1}\left(\bar\theta\right) h^k, \quad h = \frac{1}{n+1}, \tag{51}$$

and we can analytically express the constants $c_{k,1}(\bar\theta)$. More in detail, we have the following:

$$\begin{aligned} E^{\{1\}}_{\bar j_\omega,n_\omega} &= g\big(\theta_{n_\omega+1-\bar j_\omega,n_\omega}\big) - f_3\big(\theta_{\bar j_\omega+2n_\omega,n}\big) \\ &= g\left(\frac{3\pi}{10}\frac{3n_\omega+1}{n_\omega+1}\right) - f_3\left(\frac{7\pi}{10}\right) \\ &= 2\cos\left(\frac{\pi}{10}\right) - 2\cos\left(\pi\frac{\bar j_\omega}{n_\omega+1}\right). \end{aligned} \tag{52}$$

Explicitly, the errors in this example in Figure 1(d), denoted by black circles, are as follows:

$$E^{\{1\}}_{6,53} = 2\cos\left(\frac{\pi}{10}\right) - 2\cos\left(\frac{6\pi}{54}\right), \quad E^{\{1\}}_{7,63} = 2\cos\left(\frac{\pi}{10}\right) - 2\cos\left(\frac{7\pi}{64}\right),$$
$$E^{\{1\}}_{8,73} = 2\cos\left(\frac{\pi}{10}\right) - 2\cos\left(\frac{8\pi}{74}\right), \quad E^{\{1\}}_{34,333} = 2\cos\left(\frac{\pi}{10}\right) - 2\cos\left(\frac{34\pi}{334}\right),$$

and the latter relations are verified numerically to machine precision. The red circle in Figure 1(d) shows the error after applying the algorithm of Ekström et al.[9]: it reduces from $3.518 \cdot 10^{-3}$ to $-2.826 \cdot 10^{-8}$. By reformulating (52), we deduce the following:

$$E^{\{1\}}_{\tilde{j}_\omega, n_\omega} = 2\cos\left(\frac{\pi}{10}\right) - 2\cos\left(\frac{\pi}{10} + \frac{9\pi h}{5(1+2h)}\right), \tag{53}$$

and by the Taylor expansion of the error (53), we derive exactly the constants $c_{k,1}$ in (51), that is,

$$\begin{aligned}
E^{\{1\}}_{\tilde{j}_\omega, n_\omega} &= 2\cos\left(\frac{\pi}{10}\right) - \left(2\cos\left(\frac{\pi}{10}\right) + 2\sum_{k=1}^{\infty} \frac{\cos^{(k)}(\pi/10)}{k!}\left(\frac{9\pi h}{5(1+2h)}\right)^k\right) \\
&= -2\sum_{k=1}^{\infty} \frac{\cos^{(k)}(\pi/10)}{k!}\left(\frac{9\pi}{5}\right)^k h^k \left(\frac{1}{1+2h}\right)^k \\
&= -2\sum_{k=1}^{\infty} \frac{\cos^{(k)}(\pi/10)}{k!}\left(\frac{9\pi}{5}\right)^k h^k \left(\sum_{l=0}^{\infty}(-2h)^l\right)^k \\
&= -2\sum_{k=1}^{\infty} \frac{\cos^{(k)}(\pi/10)}{k!}\left(\frac{9\pi}{5}\right)^k \left(\sum_{l=0}^{\infty}(-2)^l h^{l+1}\right)^k \\
&= 2\sin(\pi/10)\left(\frac{9\pi}{5}\right)\sum_{l=0}^{\infty}(-2)^l h^{l+1} + \\
&\quad + \cos(\pi/10)\left(\frac{9\pi}{5}\right)^2\left(\sum_{l=0}^{\infty}(-2)^l h^{l+1}\right)^2 - \\
&\quad - \frac{\sin(\pi/10)}{3}\left(\frac{9\pi}{5}\right)^3\left(\sum_{l=0}^{\infty}(-2)^l h^{l+1}\right)^3 - \\
&\quad \underbrace{- 2\sum_{k=4}^{\infty} \frac{\cos^{(k)}(\pi/10)}{k!}\left(\frac{9\pi}{5}\right)^k \left(\sum_{l=0}^{\infty}(-2)^l h^{l+1}\right)^k}_{\mathcal{O}(h^4)}.
\end{aligned} \tag{54}$$

By expanding the expression in (53) up to a $\mathcal{O}(h^4)$ term, we deduce precise representations for $c_{k,1}, k = 1, 2, 3$, that is,

$$\begin{aligned}
E^{\{1\}}_{\tilde{j}_\omega, n_\omega} &= 2\sin(\pi/10)\left(\frac{9\pi}{5}\right)\underbrace{\left(h - 2h^2 + 4h^3 + \sum_{l=3}^{\infty}(-2)^l h^{l+1}\right)}_{h-2h^2+4h^3+\mathcal{O}(h^4)} + \\
&= + \cos(\pi/10)\left(\frac{9\pi}{5}\right)^2\underbrace{\left(h - 2h^2 + \sum_{l=3}^{\infty}(-2)^l h^{l+1}\right)^2}_{h^2-4h^3+\mathcal{O}(h^4)} - \\
&\quad - \frac{\sin(\pi/10)}{3}\left(\frac{9\pi}{5}\right)^3\underbrace{\left(h + \sum_{l=2}^{\infty}(-2)^l h^{l+1}\right)^3}_{h^3+\mathcal{O}(h^4)} + \mathcal{O}(h^4).
\end{aligned}$$

TABLE 1 Analytical $c_{k,1}(\bar{\theta})$, and the corresponding approximation $\tilde{c}_{k,1}(\bar{\theta})$, for m different coarse matrices in algorithm from Ekström et al.[9] for $g_3(\theta) = 2 - 2\cos(3\theta)$, $\bar{\theta} = \pi/10$

	$m = 1$ 159	$m = 2$ 159,189	$m = 3$ 159,189,219	$m = 4$ 159,189,219,249
$c_{1,1}(\bar{\theta})$	3.49489987	3.49489987	3.49489987	3.49489987
$\tilde{c}_{1,1}(\bar{\theta})$	3.63644656	3.49891734	3.49495321	3.49490028
$c_{2,1}(\bar{\theta})$		23.42262738	23.42262738	23.42262738
$\tilde{c}_{2,1}(\bar{\theta})$		22.00467555	23.39212062	23.42229454
$c_{3,1}(\bar{\theta})$			−126.29647972	−126.29647972
$\tilde{c}_{3,1}(\bar{\theta})$			−120.50951417	−126.19491717
$E^{\{1\}}_{34,333}$	$3.51819657 \cdot 10^{-3}$	$3.51819657 \cdot 10^{-3}$	$3.51819657 \cdot 10^{-3}$	$3.51819657 \cdot 10^{-3}$
$\sum_{k=1}^{m} \tilde{c}_{k,1}(\bar{\theta})h^k$	$3.63644656 \cdot 10^{-3}$	$3.52092202 \cdot 10^{-3}$	$3.51822482 \cdot 10^{-3}$	$3.51819673 \cdot 10^{-3}$
$E^{\{1\}}_{34,333} - \sum_{k=1}^{m} \tilde{c}_{k,1}(\bar{\theta})h^k$	$-1.18249995 \cdot 10^{-4}$	$-2.72544868 \cdot 10^{-6}$	$-2.82554797 \cdot 10^{-8}$	$-0.16133076 \cdot 10^{-9}$

Thus, we have the following:

$$E^{\{1\}}_{\bar{j}_\omega,n_\omega} = \underbrace{2\sin(\pi/10)\left(\frac{9\pi}{5}\right)}_{c_{1,1}(\bar{\theta})\approx 3.49489987} h + \underbrace{\left(-4\sin(\pi/10)\left(\frac{9\pi}{5}\right) + \cos(\pi/10)\left(\frac{9\pi}{5}\right)^2\right)}_{c_{2,1}(\bar{\theta})\approx 23.42262738} h^2 + \underbrace{\left(8\sin(\pi/10)\left(\frac{9\pi}{5}\right) - 4\cos(\pi/10)\left(\frac{9\pi}{5}\right)^2 - \frac{\sin(\pi/10)}{3}\left(\frac{9\pi}{5}\right)^3\right)}_{c_{3,1}(\bar{\theta})\approx -126.29647972} h^3 + \sum_{k=4}^{\infty} c_{k,1}(\bar{\theta})h^k. \tag{55}$$

Note that the explicit expressions of (55) can be derived for any combination of n, ω, and $\bar{\theta}$, but the computation will be more complicated if $\beta > 0$ because also $\tilde{\theta}^{(2)}$ has to be considered.

In Table 1, we show the results using the algorithm of Ekström et al.[9] to approximate m different constants $c_{k,1}(\bar{\theta})$ with the same number of different coarse matrices. As m increases, $\tilde{c}_{k,1}(\bar{\theta})$ converges to $c_{k,1}(\bar{\theta})$ as expected. Using the analytical expression of $c_{k,1}(\bar{\theta})$ in (55), we have $\sum_{k=1}^{3} c_{k,1}(\bar{\theta})h^k = 3.51819620 \cdot 10^{-3}$, and thus, the error after the error reduction is $E^{\{1\}}_{34,333} - \sum_{k=1}^{m} c_{k,1}(\bar{\theta})h^k = 3.67020511 \cdot 10^{-10}$.

In Table 2, we show the results obtained when using the algorithm by Ekström et al.[9] for nonmonotone cases $g_\omega(\theta) = 2 - 2\cos(\omega\theta)$ for $\omega = 2, 3, 4$: the goal is to reduce the error of the eigenvalue approximation when considering the largest matrix. The errors for $m = 0, 1, 2, 3$ different coarse matrices used to approximate the constants $c_{k,1}(\bar{\theta})$, $k = 1, \dots, m$, are presented. For $g_2(\theta)$, the coarse matrices have sizes belonging to $\{149, 189, 209\}$, and the largest size is $n = 9999$; for $g_3(\theta)$, the coarse matrices have sizes belonging to $\{159, 189, 219\}$ and $n = 10009$; for $g_4(\theta)$, the coarse matrices have sizes belonging to $\{169, 209, 249\}$ and $n = 10009$. The errors behave as expected, and hence, the algorithm taken from the work of Ekström et al.[9] can also be used for these specific nonmonotone examples, although in this setting, a numerical computation is not necessary because the exact eigenvalues can be evaluated exactly by exploiting the symbol and sampling the grid described in Section 2.

3.2 | The general symmetric banded case: conjectures and numerics

As we have seen in the previous subsection, given a positive integer $\omega \geq 2$ and the nonmonotone symbol $f(\theta) = g_\omega(\theta) = 2 - 2\cos(\omega\theta)$, and evaluating it at a equidistant grid such as $\theta_{j,n} = j\pi h, j = 1, \dots, n, h = 1/(n+1)$, numerical tests show that the error $E_n = \lambda_n - \xi_n$ can be separated into ω different types of error modes for each $\beta = \text{mod}(n, \omega)$. That is, for each $\beta = \text{mod}(n, \omega)$, there are ω disjoint subgrids of the original grid (see Figure 1 for $\omega = 3$ and the related caption). For a given n and β, each error mode is obtained by the indices $j \in I_s, s = 0, \dots, \omega - 1$, where $I_0 = \{\omega, 2\omega, 3\omega, \dots\}$ and for $s > 0$, $I_s = \{s, s + \omega, s + 2\omega, \dots\}$, and the union of all I_s forms the whole set of indices $\{1, \dots, n\}$.

TABLE 2 Errors for eigenvalue approximations for matrices with standard symbol $g\omega(\theta) = 2 - 2cos(\omega\theta)$, $\bar{\theta} = \pi/10$

$g_\omega(\theta)$	$E^{\{1\}}_{j_\omega,n_\omega}$	$E^{\{1\}}_{j_\omega,n_\omega} - \sum_{k=1}^{m} \tilde{c}_{k,1}(\bar{\theta})h^k$ $m=1$	$m=2$	$m=3$
$g_2(\theta)$	$-3.88581714\cdot10^{-5}$	$4.32478954\cdot10^{-6}$	$-5.21177503 \cdot 10^{-8}$	$-1.12193334 \cdot 10^{-9}$
$g_3(\theta)$	$34.97240870\cdot10^{-5}$	$-13.92056931 \cdot 10^{-6}$	$-38.76938472 \cdot 10^{-8}$	$-5.03491210 \cdot 10^{-9}$
$g_4(\theta)$	$65.96546126\cdot10^{-5}$	$-7.93740842 \cdot 10^{-6}$	$-127.70747416 \cdot 10^{-8}$	$-50.14789443 \cdot 10^{-9}$

The latter remark induces the conjecture that the number of the different expansions is related to the number of sign changes of the derivative of the generating function in the basic interval $(0, \pi)$, that is, a formula of the type as follows:

$$\lambda_{j,n} = f(\theta_{\sigma_n(j),n}) + \sum_{k=1}^{m} c_{k,s}\left(\theta_{\sigma_n(j),n}\right) h^k + O(h^{m+1}), \quad j \in I_s, \quad s = 0, \ldots, \omega - 1, \tag{56}$$

may hold. In Figure 2, we see a clarifying example of the nonmonotone error given by the function $f(\theta) = 2 - 2\cos(\theta) - 2\cos(2\theta)$.

In Figure 2(a), we show the true eigenvalues (sorted, solid in red) and the sampling of the symbol (unsorted, dashed in black). The two different regions displayed in light colors (red on bottom and yellow on top) represent the different number of sign changes in the derivative of the symbol $f(\theta)$ inside the region (zero and one). These different regions will give rise to different features in the behavior of the errors.

The approximation error of the function possesses the same monotone behavior as the one observed for $(2 - 2\cos(\theta))^2$, when using, for example, the grid $(j-1)\pi/(n-1)$ instead of the exact $j\pi/(n+1)$, in the interval $[0, \pi/3]$ with $f(\pi/3) = 2$, and almost the behavior typical of $2 - 2\cos(2\theta)$ in the interval $[\pi/3, \pi]$ with $f(\pi/3) = f(\pi) = 2$. Indeed, for the eigenvalues belonging to $(-2, 2]$, $-2 = f(0) = \min f$, $2 = f(\pi/3)$, as represented in the light red regions of Figure 2, the behavior of the error is like the one related with a monotone function that (56) with $\omega = 1$ holds. For the eigenvalues belonging to $(2, 17/4)$, $2 = f(\pi/3) = f(\pi)$, $17/4 = \max f$, as represented in the light yellow regions in Figure 2, the behavior of the error behaves almost like the one displayed in (56) with $\omega = 2$, because the sign of the derivative changes once.

In Figure 2(b), we present a visualization of error reduction for $f(\theta) = 2 - 2\cos(\theta) - 2\cos(2\theta)$, $\bar{\theta} = \pi/10$ with the algorithm presented by Ekström et al.[9] The largest matrix dimension is $n = 669$, whereas the coarse grids have sizes belonging to $\{109, 129, 149\}$. The black circles represent the error of symbol approximation on the corresponding grids, and the red circle is the error on the fine grid after reduction using the coarse errors. The error is reduced from $-7.899\cdot10^{-4}$ to $-9.959 \cdot 10^{-11}$. Note that here, the x-axis is ordered by the size of the true eigenvalues. The error on the left region (light red) behaves like a monotone symbol, whereas the right region (light yellow) behaves, in general terms, as a symbol of the form g_ω but with a slight shift.

As seen in Figures 2(c)–(d), the local change is somewhat drastic with a small change of n, but the general structure of the error remains as n increases. In Figure 2(c), we see the errors for $n = 200$ (solid) and $n = 202$ (dashed). Assuming two error modes for each n, note the rather large "shift" of the error curve just increasing n by a factor two. Note also that the x-axis is ordered by n and not by the size of the true eigenvalues. In Figure 2(d), we see the errors for $n = 500$ assuming two error modes. Note that the general regularity of the error in the large eigenvalues (right part of the figure) is comparable to $n = 200$ and $n = 202$ shown in Figure 2(c). In other words, the global error behavior is still regular in a weaker sense and should be investigated formally.

In Figure 3, we report the case of the error using the standard grid on the symbol $f(\theta) = 2 - 2\cos(3\theta) - 2\cos(4\theta)$. In Figure 3(a), the true eigenvalues (sorted, solid red) and the sampling of the symbol (unsorted, dashed black) are shown. Clearly, four different regions are present, colored in light red, green, blue, and yellow, depending on the number of sign changes of the derivative of the symbol in the region (zero, two, three, and one). These different regions will give rise to different characteristics of the behavior of the errors.

The error $E_{j,n} = \lambda_{j,n} - f(\theta_{\sigma_n j,n})$, for $n = 1000$, was plotted as if there are two error modes, that is, $j_1 = 1, 3, 5, \ldots$ (blue) and $j_2 = 2, 4, 6, \ldots$ (red). The light red (first) region shows the error behaving as in the monotone case, that is, the error can be reconstructed in the manner presented by Ekström et al.[9] The light yellow (fourth) part shows a clear regularity when representing the error in two sets (blue and red). On the other hand, when increasing n, we do not only decrease the error in the region but also maintain the error function, and we also change the number of "peaks", as previously demonstrated in Figure 2. In the light red region, the error behaves like a monotone symbol, and the error can be efficiently reconstructed by the same techniques as described in Section 3.1 and in Figures 1 and 2. The light green (second) and

blue (third) regions show "chaotic" behavior, resulting from the "naive" ordering of the approximated eigenvalues. Again, this behavior deserves a further study.

4 | CONCLUSIONS AND FUTURE WORK

The paper contains two types of theoretical results and a numerical part.

The first result concerns the fact that for the SST Toeplitz matrices as in (4), with $a_0, a_\omega, a_{-\omega} \in \mathbb{C}$, $0 < \omega < n$, the eigenvalues and the eigenvectors have a closed form expression. In particular, the formula for the eigenvalues $\mu_{j,n}$ in Theorem 1 is expressed in an elegant and compact way, because there exist a grid $\tilde{\theta}_n$, the one defined in (18), and the simple function $g(\theta) = a_0 + 2\sqrt{a_\omega a_{-\omega}}\cos(\theta)$ such that

$$\mu_{j,n} = g\left(\tilde{\theta}_{j,n}\right), \quad j = 1, \ldots, n.$$

Furthermore, using basic changes of variable in the integral representation of the distribution results, we show clear relationships between the symbol g and the standard generating functions of the matrices A_n, A_n^{sym}, that is, $f_\omega(\theta) = a_0 + a_\omega e^{\mathbf{i}\omega\theta} + a_{-\omega}e^{-\mathbf{i}\omega\theta}$, $g_\omega(\theta) = a_0 + 2\sqrt{a_\omega a_{-\omega}}\cos(\omega\theta)$, respectively. Also, a closed form formula for the corresponding eigenvectors is presented in Theorem 2.

The second result regards three banded Toeplitz matrices (4), with $a_0, a_\omega, a_{-\omega} \in \mathbb{R}$, $0 < \omega < n$: here, we show that an asymptotic expansion of the eigenvalues holds, with respect to the standard generating function and the usual grid (see formula (44)). The latter extends a similar asymptotic expansion holding for the eigenvalues of general symmetric real Toeplitz matrices, having polynomial cosine generating function, which is monotone on $[0, \pi]$ (see formula (3) and other works[9,15,16]): an important example of such matrices is represented by the finite-difference discretization of the operators $(-1)^q \partial^{2q}/\partial x^{2q}$, whose generating function is $(2 - 2\cos(\theta))^q$, $q \geq 1$.

The final part concerns a conjecture supported by numerical tests in which it is shown that for a generic banded real symmetric Toeplitz matrix, the eigenvalue $\lambda_{j,n}$ compared with $f\left(\theta_{\sigma_n j,n}\right)$ either shows an expansion similar to formula (44) if $\lambda_{j,n} \in [m, M]$ and $f'(\theta)$ has ω changes of sign for $f(\theta) \in [m, M]$ or shows an expansion like formula (3) if $\lambda_{j,n} \in [m, M]$ and $f(\theta) \in [m, M]$ is monotone.

The latter gives the ground for extrapolation techniques[24] for computing the eigenvalues of large banded real symmetric Toeplitz matrices in a fast way. Of course, also the multidimensional and the block cases should be considered and explored in future works, owing to their importance in the numerical approximation of (systems of) partial differential equations.

ACKNOWLEDGEMENTS

The authors would like to thank their families, colleagues, and friends for fruitful discussions and insights. The research of the first author is funded by the Graduate School in Mathematics and Computing (FMB) and Uppsala University, and the second author is supported by the Italian Group of Scientific Computing INDAM-GNCS.

ORCID

S.-E. Ekström http://orcid.org/0000-0002-7875-7543

S. Serra-Capizzano http://orcid.org/0000-0001-9477-109X

REFERENCES

1. Böttcher A, Silbermann B. Introduction to large truncated Toeplitz matrices. New York: Springer-Verlag; 1999.
2. Serra-Capizzano S. On the extreme eigenvalues of Hermitian (block) Toeplitz matrices. Linear Algebra Appl. 1998;270:109–129.
3. Grenander U, Szegő G. Toeplitz forms and their applications. 2nd ed. New York: Chelsea; 1984.
4. Tilli P. A note on the spectral distribution of Toeplitz matrices. Linear Multil Algebra. 1998;45(2/3):147–159.
5. Tyrtyshnikov E. A unifying approach to some old and new theorems on distribution and clustering. Linear Algebra Appl. 1996;232:1–43.
6. Serra-Capizzano S, Bertaccini D, Golub G. How to deduce a proper eigenvalue cluster from a proper singular value cluster in the nonnormal case. SIAM J Matrix Anal Appl. 2005;27(1):82–86.
7. Bini D, Capovani M. Spectral and computational properties of band symmetric Toeplitz matrices. Linear Algebra Appl. 1983;52/53:99–126.
8. Bogoya J, Böttcher A, Maximenko E. From convergence in distribution to uniform convergence. Bol Soc Mat Mex. 2016;3(22):695–710.

9. Ekström S-E, Garoni C, Serra-Capizzano S. Are the eigenvalues of banded symmetric Toeplitz matrices known in almost closed form? Exp Math. 2017. https://doi.org/10.1080/10586458.2017.1320241
10. Serra-Capizzano S. On the extreme spectral properties of Toeplitz matrices generated by L1 functions with several minima/maxima. BIT. 1996;36(1): 135–142.
11. Stein EM, Weiss G. Introduction to Fourier analysis on Euclidean spaces. Princeton, NJ: Princeton University Press; 1971.
12. Bogoya J, Grudsky S, Maximenko E. Eigenvalues of Hermitian Toeplitz matrices generated by simple-loop symbols with relaxed smoothness. Oper Theory Adv Appl. 2017;259:179–212.
13. Ahmad F, Al-Aidarous E, Alrehaili D, Ekström S-E, Furci I, Serra-Capizzano S. Are the eigenvalues of preconditioned banded symmetric Toeplitz matrices known in almost closed form? Numer Algoritm 1–27, 2017. In press.
14. Ekström S-E, Furci I, Serra-Capizzano S. Are the Eigenvalues of the B-spline IgA approximation of $-\Delta u = \lambda u$ known in almost closed form? 2017. TR Division of Scientific Computing, IT Department, Uppsala University. http://www.it.uu.se/research/publications/reports/2017-016
15. Bogoya J, Böttcher A, Grudsky S, Maximenko E. Eigenvalues of Hermitian Toeplitz matrices with smooth simple-loop symbols. J Math Anal Appl. 2015;422(2):1308–1334.
16. Böttcher A, Grudsky S, Maximenko E. Inside the eigenvalues of certain Hermitian Toeplitz band matrices. J Comput Appl Math. 2010;233(9): 2245–2264.
17. Böttcher A, Grudsky S. Spectral properties of banded Toeplitz matrices. Philadelphia: SIAM; 2005.
18. Elliott JF. The characteristic roots of certain real symmetric matrices [master's thesis]. Knoxville: University of Tennessee; 1953. http://trace.tennessee.edu/utk_gradthes/2384
19. Gantmakher FR, Krein MG. Ostsilliatsionnye matritsy i iadra i malye kolebaniia mekhanicheskikh sistem (Oscillation matrices and kernels and small vibrations of mechanical systems). Soviet Union: Gostekhizdat; 1950.
20. Noschese S, Pasquini L, Reichel L. Tridiagonal Toeplitz matrices: Properties and novel applications. Numer Linear Algebra Appl. 2013;20(2):302–326.
21. Smith GD. Numerical solution of partial differential equations: Finite difference methods. 2nd ed. Oxford: Clarendon Press; 1978.
22. Ekström S-E, Serra-Capizzano S. Eigenvalues and eigenvectors of banded Toeplitz matrices and the related symbols. 2017. TR Division of Scientific Computing, IT Department, Uppsala University. http://www.it.uu.se/research/publications/reports/2017-010/
23. Tyrtyshnikov E, Zamarashkin N. Spectra of multilevel Toeplitz matrices: Advanced theory via simple matrix relationships. Linear Algebra Appl. 1998;270:15–27.
24. Brezinski C, Redivo Zaglia M. Extrapolation methods theory and practice, studies in computational mathematics. 2nd ed. Amsterdam: North-Holland Publishing Co; 1991.

How to cite this article: Ekström S-E, Serra-Capizzano S. Eigenvalues and eigenvectors of banded Toeplitz matrices and the related symbols. *Numer Linear Algebra Appl*. 2018;25:e2137. https://doi.org/10.1002/nla.2137